High Island Densities in Pulsed Laser Deposition: Causes and Implications

M. Schmid, C. Lenauer, A. Buchsbaum, F. Wimmer, G. Rauchbauer, P. Scheiber, G. Betz, and P. Varga

Institut für Allgemeine Physik, Technische Universität Wien, 1040 Wien, Austria

(Received 11 May 2009; published 10 August 2009)

By studying metal growth on Pt(111), we determine the reasons for the high island densities observed in pulsed laser deposition (PLD) compared to conventional thermal deposition. For homoepitaxy by PLD with moderate energies ($\lesssim$100 eV) of the deposited ions, high island densities are caused by the high instantaneous flux of arriving particles. Additional nuclei are formed at high ion energies ($\gtrsim$200 eV) by adatoms created by the impinging ions. For heteroepitaxy, the island density is also increased by intermixing (deposited material implanted in the surface), creating an inhomogeneous potential energy surface for diffusing atoms. We discuss implications for layer-by-layer growth and sputter deposition.

DOI: 10.1103/PhysRevLett.103.076101 PACS numbers: 81.15.Fg, 68.55.A−, 81.15.Aa, 81.15.Ef

Pulsed laser deposition (PLD) is a versatile technique for growing films of almost any material and offers significant advantages over conventional thermal deposition (TD) such as improved layer-by-layer growth and stoichiometric transfer of material from the target to the substrate [1–3]. For PLD, pulses of an energetic laser are directed onto a target; the typical fluence (energy density) is few J/cm^2 for 10–30 ns pulses. The ablated material forms a plasma plume, and, depending on the laser fluence, the ejecta deposited on the substrate contain a large fraction of singly or multiply charged ions with energies between tens and hundreds of eV. This is 2 to 3 orders of magnitude above the particle energies in TD.

When comparing TD and PLD, one of the most obvious features of PLD-grown films is the high island density. Many groups attribute this fact to the high instantaneous flux of particles arriving on the substrate after each laser pulse [3]. According to nucleation theory [4–7], this increases the island density. Other works also show that the energy of the impinging ions plays an important role (Fe/Cu(111), [8]) and a further study found a significantly enhanced diffusion rate for PLD, attributed to energetic particles (Fe/Mo(110), [9]). For Co/Cu(100), identical island densities for TD and PLD have been reported, questioning these results [10]. Concerning improved layer-by-layer growth, it was concluded that deposition in pulses is insufficient to explain it [11]; disruption of islands by impinging energetic ions [2] was proposed as a reason. Even for simple systems like metal-on-metal growth, no coherent picture emerges, and the reasons for the differences between TD and PLD remain obscure. Our study for the first time combines atomic-scale observations of nucleation in PLD and measurements of the ion energies, making it possible to disentangle the different effects.

Experiments were conducted in a two-chamber ultrahigh vacuum system; base pressures in the preparation and STM (scanning tunneling microscopy) chambers are in the mid-10^{-11} and upper 10^{-12} mbar range, respectively. The substrate, a Pt(111) single crystal, was cleaned by cycles of sputtering (3 keV Ar^+) and annealing ($\approx$800 °C), stored in the STM chamber until shortly before deposition and placed on a manipulator cooled by liquid nitrogen ($T > 100$ K) or liquid He ($T < 100$ K) for deposition (temperature accuracy $\approx \pm 10$ K at low T). No impurities could be detected by Auger electron spectroscopy; STM showed a very small concentration [$\approx 10^{-3}$–10^{-4} monolayers (ML)] of oxygen. For PLD, the beam of a frequency-doubled Nd:YAG laser (532 nm) with 10 ns pulse length

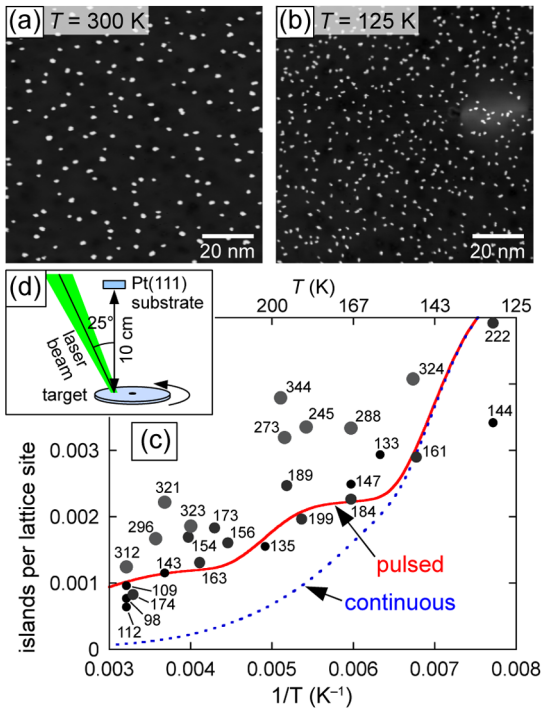

FIG. 1 (color online). (a),(b) STM images of 0.014 ML Pt deposited on Pt(111) by PLD (STM at 80 K). (c) Experimental island densities labeled with the energies of the impinging Pt ions. Full and broken lines show calculated island densities for pulsed (10 pulses, 10 μs each, 10 Hz) and continuous (1 s) deposition. (d) Geometry of our PLD setup.

and 10 Hz repetition frequency was focused onto a rotating target [polycrystalline Pt or Co; see Fig. 1(d) for the geometry]. The energy distribution of the ablated ions was measured by a time-of-flight spectrometer; the fraction of neutrals with a lower energy was found to be negligible [12]. The ion energy, which increases with increasing laser fluence on the target, was varied by changing the focus size and pulse energy, keeping the deposition rate constant [13]; the fluence required for 100 eV Pt^+ ion energy was about 1.5–2 J/cm^2. The deposition rate was determined by a temperature-controlled quartz crystal microbalance operated at the minimum of its frequency-versus-temperature curve; and the laser was operated continuously with constant pulse energy between rate determination and deposition to ensure high rate accuracy. Nevertheless, pulse-to-pulse fluctuations of the laser as well as small inhomogeneities of the target lead to fluctuations of the amount of ablated material in a single pulse. For depositing low amounts of material, we have therefore not used single pulses but 10 successive laser pulses, resulting in an estimated accuracy of the coverage better than $\pm 20\%$ with the exception of conditions very close to the ablation threshold, where pulse-to-pulse fluctuations of the ablation yield are very large. The rate was also checked by deposition of larger amounts of material and measuring the island areas by STM.

For calculating Pt/Pt(111) island densities, we have used nucleation theory with rate equations as in Ref. [5], but including dimer mobility. We have used monomer and dimer diffusion barriers of 0.26 and 0.37 eV, respectively, preexponential factors of 5×10^{12} s^{-1} [14], capture numbers of 3 for monomers and dimers [5], and coverage-dependent capture numbers [7] for larger islands. These values perfectly reproduce the island density obtained by thermal deposition [6] in the temperature range of interest. The calculations include a post-deposition period of 200 s with the sample at the deposition temperature before insertion into the STM, where the temperature was low enough to prevent further diffusion.

Figures 1(a) and 1(b) show STM images of 0.014 ML Pt deposited at different temperatures by 10 pulses on Pt(111). The island densities obtained from such experiments are shown in Fig. 1(c). Besides the usual increase of island density with decreasing temperature, it is obvious that higher energies of the impinging Pt ions (larger and lighter disks) lead to higher island densities than lower ion energies. Figure 1(c) also shows island densities calculated with nucleation theory for pulsed deposition (assuming particles arriving in 10-μs-pulses; this time spread is due to the distribution of flight velocities between target and sample). Considering the experimental errors, this curve agrees well with the measured island densities for low and moderate ion energies. For temperatures above $\approx$150 K, where the time needed for the formation of stable nuclei from single adatoms is shorter than the time between two laser pulses, the island density calculated for pulsed deposition is higher than for continuous deposition with the same average deposition rate: Immediately after the pulses, the adatom density n_1 is significantly higher than for continuous deposition. As the rate of dimer formation is proportional to n_1^2, this leads to an increased density of nuclei. Similarly, the second plateau of the island density at $\approx$250 K is related to dimer diffusion; there the high instantaneous dimer density n_2 after a pulse results in more adatom-dimer and dimer-dimer mergers than in continuous deposition. Adatom diffusion within the $\approx$10 μs deposition periods plays a role only at temperatures above $\approx$ 270 K; the influence of the exact deposition period on the island density is very small.

While we could explain the island densities for ion energies below $\approx$150 eV by standard nucleation theory, taking pulsed deposition into account, the island densities for ion energies above $\approx$200 eV are clearly higher than calculated. To examine the reasons for this, we have deposited 0.0056 ML Pt at temperatures below 60 K (where adatom diffusion is frozen) and measured the resulting adatom density at 5 K. The substrate lattice could be reconstructed from a few CO molecules in the images, knowing that these are in on-top sites. The STM images [Figs. 2(a) and 2(b)] show mostly single Pt adatoms in fcc hollow sites. A few species appear as double maxima in adjacent fcc and hcp sites [above center in Fig. 2(b)]. We

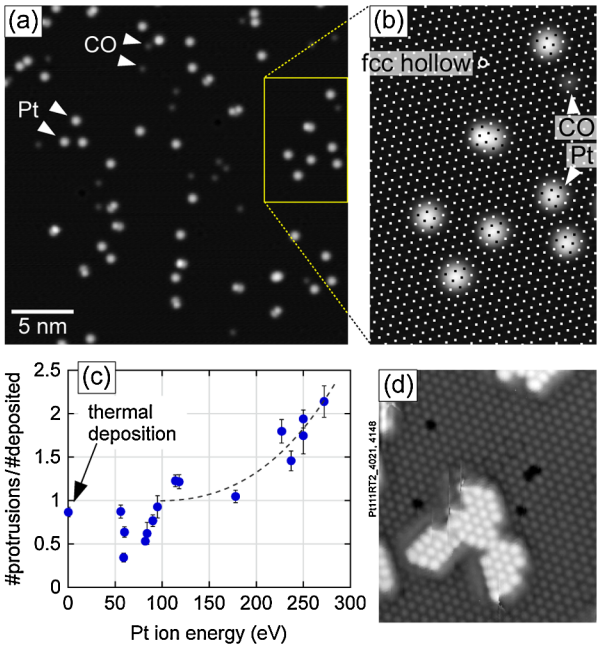

FIG. 2 (color online). (a) STM image of 0.0056 ML Pt deposited on Pt(111) by PLD at 50 K (E_{ion} = 90 eV; STM at 5 K). The Pt(111) substrate lattice reconstructed from the CO sites is superimposed on (b). (c) Number of adatoms or clusters depending on the energy of the impinging Pt ions. 2σ error bars include counting statistics only. The broken line is a guide to the eye. (d) STM image of 0.2 ML deposited at 180 K (E_{ion} = 130 eV), showing vacancies in the substrate. The image was processed for better visibility of the atomic corrugation on the substrate and adatom islands.

attribute these to Pt adatoms having trapped an adsorbate mobile at 50 K, possibly H_2O. For thermal deposition and at ion energies around 100 eV, we find roughly one adatom per deposited Pt atom/ion, whereas ion energies between 200 and 300 eV lead to roughly two adatoms per deposited Pt [Fig. 2(c)]. The data below 100 eV are close to the ablation threshold and thus suffer from large rate uncertainties. Our observations of more than one adatom per deposited atom can be easily explained as it is known that impinging ions not only eject target atoms from the surface (sputtering), but also push atoms out of the surface with lower kinetic energy and thereby create adatoms [15]. We call this effect "failed sputtering." We have performed molecular dynamics calculations with the same potentials as in Ref. [16]; the calculated adatom yield is higher than the sputter yield by 1–2 orders of magnitude: 2.2 adatoms and 0.05 sputtered atoms per impinging 100 eV Pt^+. The calculations do not include inelastic losses and therefore overestimate the adatom yield [16]; annihilation of nearby adatom-vacancy pairs may further reduce the number of adatoms if the barrier for this process is ≤ 0.1 eV. Our experimental data are more comparable to the experimental adatom yield of 1.6 for 200 eV Xe $\rightarrow$ Pt(111) [17].

Failed sputtering also results in vacancies in the surface. Vacancies and vacancy clusters can be observed by STM also at higher temperatures [Fig. 2(d)], and we also noticed that their number increases with ion energy. Vacancy clusters were observed even at room temperature. This means that some of the adatoms caused by failed sputtering do not fall victim to adatom-vacancy annihilation; thus, these adatoms contribute to nucleation and thereby increase the island density also at higher temperatures. The increase of island densities above that obtained from nucleation theory [Fig. 1(c)] occurs in the same energy range as the increase of the adatom yield [Fig. 2(c)], confirming our hypothesis that failed sputtering is responsible for the increased island density.

In heteroepitaxy or when depositing compounds, intermixing of substrate and deposited material comes in as an additional factor [8,18]. As a model system, we have used deposition of Co on Pt(111). Chemical contrast allows us to discriminate between Pt and Co in the first layer; vacancies appear much darker than Co atoms embedded in the first monolayer [Fig. 3(a)]. For ion energies around 80 eV, we find that the average surface concentration of Co is $\approx 30\%$ of the deposited coverage; i.e., about every third Co atom is implanted into the surface. Looking at the island sizes [Figs. 3(b) and 3(c)], we find a very obvious difference between Co/Pt(111) PLD on the one hand and PLD of Pt/Pt(111) or TD of any material on Pt(111): While TD and homoepitaxial growth by PLD yield "normal" island size distributions [19], PLD of Co on Pt(111) results in a wider island size distribution, with many small islands, in contrast to the distribution expected for the critical nucleus size of $i^* = 2$ found by TD at 300 K [20], but also incompatible with $i^* = 1$. We can explain this by heterogeneous nucleation on sites with implanted

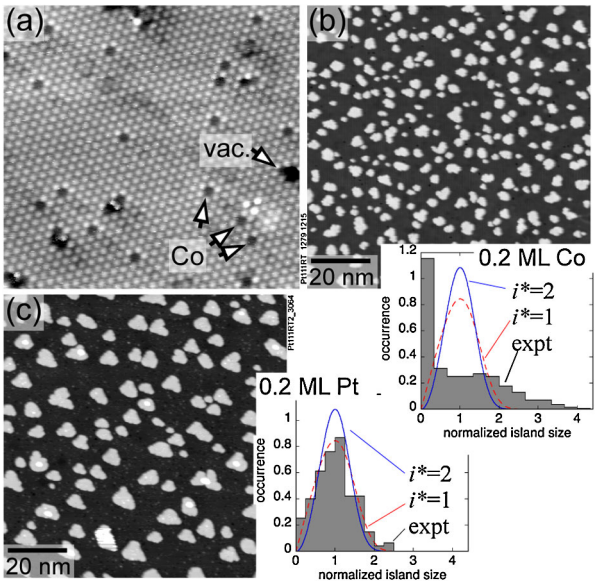

FIG. 3 (color online). STM images of (a),(b) 0.2 ML Co and (c) 0.2 ML Pt deposited on Pt(111) by PLD at 300 K. The insets show experimental (813 and 189 islands for Co and Pt, respectively) and calculated [19] island size distributions.

Co, i.e., a higher corrugation of the potential energy landscape than on a pure-metal surface [21]. With increasing Co coverage, new nucleation sites are formed by implantation of Co on the terraces during deposition; islands nucleating on these sites have less time to grow and more competitors for adatoms than those nucleating earlier, explaining the extra peak at very low island sizes. Without the formation of additional nuclei, the final island density is reached soon after nucleation, leading to a narrower size distribution. As the small (young) islands are often far from larger (older) ones, they cannot be attributed to breakup of islands by impinging energetic particles as proposed in Ref. [2]. The breakup mechanism would also apply for both homo and heteroepitaxy, while we observe unusual island size distributions in heteroepitaxy only.

What is the significance of our findings for layer-by-layer growth? Increased nucleation density alone usually does not improve layer-by-layer growth (unless nuclei are created at the right moment, after the previous layer has been closed [22]). For example, considering the dependence on the flux F and assuming immobile dimers (critical nucleus $i^* = 1$), the island density is proportional to $F^{1/3}$, and the minimum density of islands necessary to suppress second-layer nucleation (at a given coverage) is $\propto 1/R_{\mathrm{crit}}^2 \propto F^{-2/7}$ [6]. The remaining factor of $F^{1/21}$ could tip the balance towards layer-by-layer growth only in rare cases that are very close to layer-by-layer growth at low flux. The situation is different for very small islands: Atoms implanted with moderate energy will simply push island atoms onto the bare terrace. Thus, no adatom is created on the island, and second-layer nucleation does not take place. This nicely explains why we find the best

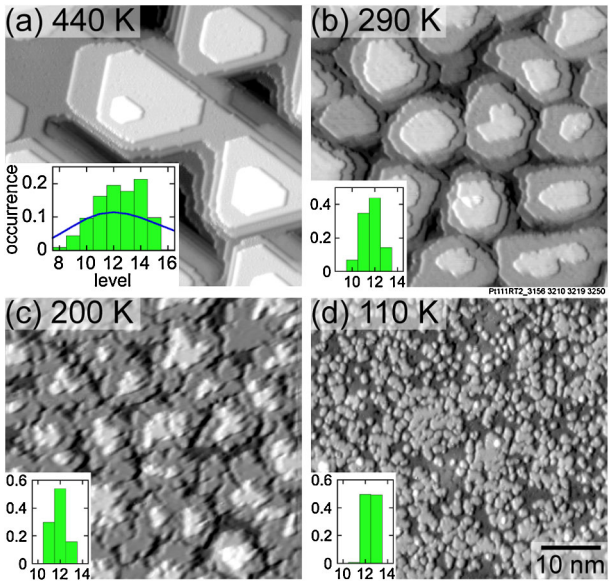

FIG. 4 (color online). STM images of 12 ± 1 ML Pt deposited on Pt(111) by PLD at ≈100 eV kinetic energy (shown as if illuminated from the left). Insets show height distributions; the curve in (a) is the Poisson distribution arising in case of no interlayer mass transport.

layer-by-layer growth of Pt on Pt(111) at 110 K, where islands are in the 1 nm range (Fig. 4). An analysis of Fig. 4(d) shows that ≈90% of the island area is within two interatomic distances from the border, i.e., in the range where it is likely that deposition with moderate particle energies will result in implantation without any adatoms remaining. For larger islands (higher T), the height distributions show more than two levels; i.e., islands grow on top of other islands.

In summary, the high island densities in homoepitaxy are mainly due to the high instantaneous flux of impinging atoms or ions, but further increased by adatom creation (failed sputtering) at high energies of the impinging ions (high laser fluence). For heteroepitaxy, the chemically heterogeneous surface created by implantation leads to a further increase of the island density. We expect a similar mechanism also for compounds and oxides, though there the variety of ''chemical'' defects created by impinging ions is obviously larger. High island densities imply small islands, where easy implantation near the edges facilitates layer-by-layer growth.

Among all deposition methods, PLD is only a niche player, but it has the advantage of being experimentally far more accessible than the widely used method of sputter deposition. Our results on the influence of different particle energies can be applied for this method as well. It has been shown that energetic particles in a sputtering setup lead to increased island densities [23]. Our data confirm the conclusions drawn there by showing that particle energies well above 100 eV are needed for creation of additional nuclei by failed sputtering; these energies are only reached by gas ions neutralized and reflected at the cathode, not by sputtered target atoms. Intermixing between deposited material and the substrate occurs at lower energies, however, and also causes increased island densities in chemically heterogeneous systems. Improved layer-by-layer growth due to atom implantation near the edges is also possible in the energy range reached by sputtered atoms, in case of small islands.

We would like to thank Georg Kresse for density functional theory calculations telling us that the fcc-hcp pairs cannot be Pt_2 dimers. This work was supported by the Austrian *Fonds zur Förderung der wissenschaftlichen Forschung*, Project No. P17728.

[1] *Pulsed Laser Deposition of Thin Films*, edited by D. B. Chrisey and G. K. Hubler (Wiley, New York, 1994).
[2] P. R. Willmott *et al.*, Phys. Rev. Lett. **96**, 176102 (2006).
[3] H. Jenniches *et al.*, Phys. Rev. B **59**, 1196 (1999).
[4] J. A. Venables, G. D. T. Spiller, and M. Hanbücken, Rep. Prog. Phys. **47**, 399 (1984).
[5] H. Brune, Surf. Sci. Rep. **31**, 125 (1998).
[6] T. Michely and J. Krug, *Islands, Mounds and Atoms: Patterns and Processes in Crystal Growth Far from Equilibrium* (Springer, Berlin, 2004).
[7] J. A. Venables, Philos. Mag. **27**, 697 (1973).
[8] H. Schiechl, G. Rauchbauer, A. Biedermann, M. Schmid, and P. Varga, Surf. Sci. **594**, 120 (2005).
[9] P.-O. Jubert, O. Fruchart, and C. Meyer, Surf. Sci. **522**, 8 (2003).
[10] C. Tröppner, A. Dobler, and T. Fauster, Verh. Dtsch. Phys. Ges. (VI) **42**, 568 (2007).
[11] B. Hinnemann, H. Hinrichsen, and D. E. Wolf, Phys. Rev. E **67**, 011602 (2003).
[12] A. Buchsbaum, G. Rauchbauer, P. Varga, and M. Schmid, Rev. Sci. Instrum. **79**, 043301 (2008).
[13] G. Rauchbauer, A. Buchsbaum, H. Schiechl, P. Varga, M. Schmid, and A. Biedermann, Surf. Sci. **602**, 1589 (2008).
[14] C. Busse *et al.*, Surf. Sci. **539**, L560 (2003).
[15] T. Michely and G. Comsa, Phys. Rev. B **44**, 8411 (1991).
[16] H. Gades and H. M. Urbassek, Phys. Rev. B **50**, 11167 (1994).
[17] T. Michely and C. Teichert, Phys. Rev. B **50**, 11156 (1994).
[18] M. Störmer *et al.*, Appl. Phys. A **69**, S455 (1999).
[19] J. G. Amar and F. Family, Phys. Rev. Lett. **74**, 2066 (1995).
[20] R. Kalousek *et al.*, Phys. Rev. B **68**, 233401 (2003).
[21] Direct observation by STM shows that all single Pt adatoms on Pt(111) become mobile below 85 K. On a Pt(111) surface with embedded Co, we find stationary Pt even at 120 K.
[22] G. Rosenfeld, R. Servaty, C. Teichert, B. Poelsema, and G. Comsa, Phys. Rev. Lett. **71**, 895 (1993).
[23] M. Kalff, M. Breeman, M. Morgenstern, T. Michely, and G. Comsa, Appl. Phys. Lett. **70**, 182 (1997).